PHYSICAL REVIEW A, VOLUME 64, 033609

Laser probing of Cooper-paired trapped atoms

G. M. Bruun,[1] P. Törmä,[2] M. Rodriguez,[2] and P. Zoller[3]
[1]*Nordita, Blegdamsvej 17, 2100 Copenhagen, Denmark*
[2]*Laboratory of Computational Engineering, P.O. Box 9400, FIN-02015 Helsinki University of Technology, Finland*
[3]*Institute for Theoretical Physics, University of Innsbruck, Technikerstraße 25, A-6020 Innsbruck, Austria*
(Received 16 November 2000; published 16 August 2001)

We consider a gas of trapped Cooper-paired fermionic atoms that are manipulated by laser light. The laser induces a transition from an internal state with large negative scattering length (superfluid) to one with weaker interactions (normal gas). We show that the process can be used to detect the presence of the superconducting order parameter. Also, we propose a direct way of measuring the size of the gap in the trap. The efficiency and feasibility of this probing method is investigated in detail in different physical situations.

DOI: 10.1103/PhysRevA.64.033609 PACS number(s): 03.75.Fi, 05.30.Fk, 32.80.−t

I. INTRODUCTION

Recent experiments on cooling and trapping fermionic atoms have opened up new opportunities for studying fundamental quantum statistical and many-body physics. Trapped fermionic ^{40}K atoms were cooled down to temperatures at which the Fermi degeneracy sets in [1]. Two lithium isotopes were trapped simultaneously in a magneto-optical trap in [2] and optical trapping of fermionic lithium has been achieved as well [3]. The richness of the internal energy structure of the atoms and the possibility to accurately and efficiently manipulate these energy states by laser light and magnetic fields allow excellent control of these gases. Furthermore, atomic gases are dilute and weakly interacting, thus offering the ideal tool for developing and experimentally testing theories of many-body quantum physics.

The degenerate Fermi gas is expected to show many interesting phenomena in its thermodynamics [4], excitation spectrum [5–8], collisional dynamics [9], and scattering of light [1,10,11]. A major goal is to observe the predicted [12,13] BCS transition for fermionic atoms; this would compare to the experimental realization of atomic Bose-Einstein condensates [14]. It is still, however, an open question how to observe the BCS transition, because the value of the superconducting order parameter (gap) is expected to be small and the existence of the order parameter does not significantly change the density profile and other bulk properties of the gas.

There are several proposals for measuring the superconducting order parameter. Off-resonant light scattering as a probe was proposed in [15,16]. Superfluidity is predicted to effect both the spectral and spatial distribution of the scattered light. In [17], superfluidity was found to increase the optical line shift and linewidth. Also nonoptical phenomena, such as collective and single-particle excitations, have been proposed to be used for observing the BCS transition [18–22]. Probing by a magnetic field was considered in [23].

The use of on-resonant light as a probe for the order parameter was proposed in [24]. The basic idea is to transfer atoms from one internal (hyperfine) state for which the atoms are Cooper-paired to another state for which the interatomic interaction is not strong enough to lead to a BCS state. This effectively creates a superconducting—normal state interface across which the atomic population can move. There is a conceptual analogy to electron tunneling from a superconducting metal to a normal one that is used to measure the gap and the density of states for Cooper-paired electrons [25]. The tunability of the interaction strengths that is required for this scheme is obtained by the use of magnetic fields. This allows us to manipulate the scattering lengths between atoms in different internal states; see, e.g., the recent experimental results concerning optically trapped fermionic lithium atoms [3] and the theoretical predictions for ^{40}K [26].

The basic idea in the proposal [24] is that the absorption peak is shifted and becomes asymmetric because of the existence of the gap; the laser has to provide energy for breaking the Cooper pairs in order to transfer atoms from the paired state to the unpaired one. This behavior is, however, strongly influenced by the specific physical situation. In this paper, we investigate in detail how the choice of chemical potentials for the superfluid and the normal state, and the choice of the interaction strengths and laser profiles, affect the absorption. We also compare the results in the cases of a homogeneous system and a trapped gas. In Sec. II, we introduce the considered system. The linear response of the gas for a light probe is derived in Sec. III, both for a homogeneous and a trapped gas. In Sec. IV, the various parameters that affect the observed absorption are discussed. In Sec. V, numerical results are presented for the limit when the laser beam profile can be considered a constant. A beam profile with nonzero intensity only in a small volume in the middle of the trap is considered in Sec. VI. This case is very interesting because then only the center of the trap is probed. Thus the order parameter seen by the laser is almost constant, and indeed we find a remarkable agreement with the results predicted for a homogeneous system. We finally summarize the results in Sec. VII.

II. THE SUPERCONDUCTOR–NORMAL STATE INTERFACE

We consider atoms with three internal states available, say $|e\rangle$, $|g\rangle$, and $|g'\rangle$. They are chosen so that the interaction between atoms in states $|g\rangle$ and $|g'\rangle$ is relatively strong and

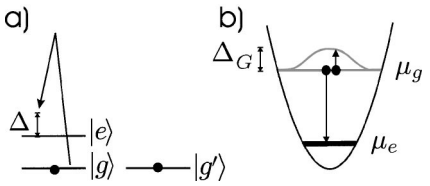

FIG. 1. Probing of the gap in a gas of attractively interacting cold fermionic atoms. (a) Laser excitation with the coupling Ω and the detuning Δ transfers a Cooper-paired atom from the internal state $|g\rangle$ to the state $|e\rangle$. (b) The other atom in the initial Cooper pair becomes an excitation in the BCS state, therefore the laser must also provide the additional gap energy Δ_G. In this picture, the Fermi levels μ_g and μ_e for the internal states have been chosen to be different from each other but they could also be equal.

their chemical potentials are nearly equal so that $|g\rangle$ and $|g'\rangle$ can be assumed to be Cooper-paired. All other interactions are small enough and/or the chemical potentials of the corresponding states are different enough in order to assume that the $|e\rangle$ atoms are in a normal state [12]. The laser frequency is chosen to transfer the population between $|e\rangle$ and $|g\rangle$, but is not in resonance with any transition that could move population away from the state $|g'\rangle$.

For small intensities, the laser interaction can be treated as a perturbation, the unperturbed states being the normal and the superconducting state. The transfer of atoms from $|g\rangle$ to $|e\rangle$ is then analogous to tunneling of electrons from a normal metal to a superconductor induced by an external voltage, which can be used as a method to probe the gap and the density of states of the superconductor [25]. In our case, the tunneling is between two internal states rather than two spatial regions. This resembles the idea of internal Josephson oscillations in two-component Bose-Einstein condensates [27]. Figure 1 illustrates the basic idea. The observable carrying essential information about the superconducting state is the change in the population of the state $|e\rangle$, we call this the current I.

We define a two-component fermion field,

$$\psi(\mathbf{x})=\begin{pmatrix}\psi_e(\mathbf{x})\\ \psi_g(\mathbf{x})\end{pmatrix}, \tag{1}$$

where ψ_e and ψ_g fulfill standard fermionic commutation relations. The fields $\psi_{e/g}$ can be expanded using some basis functions (e.g., plane waves or trap wave functions) and corresponding creation and annihilation operators: $\psi_{e/g}(\mathbf{x})=\sum_j c_j^{e/g}\phi_j^{e/g}(\mathbf{x})$. The annihilation and creation operators fulfill $\{c_i^{e\dagger},c_j^{g}\}=0$ and $\{c_i^{e/g\dagger},c_j^{e/g}\}=\delta_{ij}$. The two components of the field, corresponding to the internal states $|e\rangle$ and $|g\rangle$, are coupled by a laser. This can be either a direct excitation or a Raman process; we denote the atomic energy level difference ω_a ($\hbar\equiv 1$), the laser frequency ω_L, and the wave vector k_L; in the case of a Raman process, these are effective quantities. In the rotating-wave approximation, the Hamiltonian reads

$$H=H_e+H_{gg'}+\frac{\Delta}{2}\int d^3x\,\psi^\dagger(\mathbf{x})\sigma_z\psi(\mathbf{x}) + \int d^3x\,\psi^\dagger(\mathbf{x})\begin{pmatrix}0 & \Omega(\mathbf{x})\\ \Omega^*(\mathbf{x}) & 0\end{pmatrix}\psi(\mathbf{x}). \tag{2}$$

Here $\Delta=\omega_a-\omega_L$ is the (effective) detuning and $\Omega(\mathbf{x})$ contains the spatial dependence of the laser field multiplied by the (effective) Rabi frequency. The Hamiltonian for the $|g\rangle$ and $|g'\rangle$ atoms reads

$$H_{gg'}=\int d\mathbf{x}\sum_{\alpha=g,g'}\Big[\psi_\alpha^\dagger(\mathbf{x})\Big(-\frac{\nabla^2}{2m}+U_0(\mathbf{x}) + g_{e\alpha}\langle\psi_e^\dagger(\mathbf{x})\psi_e(\mathbf{x})\rangle-\mu_\alpha\Big)\psi_\alpha(\mathbf{x})\Big] + g_{gg'}\int d\mathbf{x}\,\psi_g^\dagger(\mathbf{x})\psi_{g'}^\dagger(\mathbf{x})\psi_{g'}(\mathbf{x})\psi_g(\mathbf{x}), \tag{3}$$

where $g_{gg'}=4\pi a_{gg'}/m$ is the interaction potential for s-wave scattering between particles in the states $|g\rangle$ and $|g'\rangle$, and $g_{e\alpha}=4\pi a_{e\alpha}/m$ is that between $|e\rangle$ and $|g\rangle$ or $|g'\rangle$; $a_{gg'}$ and $a_{e\alpha}$ are the corresponding s-wave scattering lengths. The interaction of the $|g\rangle$ and $|g'\rangle$ atoms with the $|e\rangle$ atoms is treated within the mean-field (Hartree) approximation. Using the usual BCS theory, the last line of Eq. (3) decomposes into two kinds of terms: (i) those that lead to potential terms of the Hartree field form $W(\mathbf{x})=g_{gg'}\langle\psi_g^\dagger(\mathbf{x})\psi_g(\mathbf{x})\rangle$, and (ii) contributions that produce the superconducting order parameter (gap) $\Delta_G(\mathbf{x})$. Care has to be taken when calculating $\Delta_G(\mathbf{x})$ because of the renormalization of the interaction potential (for more details, see [28]). The possible spatial inhomogeneity, e.g., from the trap potential is contained in $U_0(\mathbf{x})$, and μ_α are the chemical potentials. The Hamiltonian for the e state is given by

$$H_e=\int d\mathbf{x}\,\psi_e^\dagger(\mathbf{x})\Big(-\frac{\nabla^2}{2m}+U_0(\mathbf{x})-\mu_e + \sum_{\alpha=g,g'}g_{e\alpha}\langle\psi_\alpha^\dagger(\mathbf{x})\psi_\alpha(\mathbf{x})\rangle\Big)\psi_e(\mathbf{x}). \tag{4}$$

III. THE CURRENT

The observable carrying essential information about the superconducting state is the rate of change in population of the $|e\rangle$ state. We may call it, after the electron tunneling analogy, the current

$$I(t)=-\langle\dot{N}_e\rangle,$$

where $N_e=\int d^3x\,\psi_e^\dagger(\mathbf{x})\psi_e(\mathbf{x})$. The current $I(t)$ is calculated considering the tunneling part of the Hamiltonian,

$$H_T=H-[H_e+H_{gg'}+\Delta/2(N_e-N_g)], \tag{5}$$

as a perturbation; the current I becomes the first-order response to the external perturbation caused by the laser. We

calculate it both in the homogeneous case and in the case of harmonic confinement. The calculations are done in the grand-canonical ensemble, therefore the chemical potentials μ_g and μ_e are introduced. They are defined as the derivatives of the free energy with respect to the number of atoms in the states $|g\rangle$ and $|e\rangle$, respectively. Also the detuning Δ acts like a difference in chemical potentials, thus it becomes useful to define an effective quantity of the form $\tilde{\Delta}=\mu_e-\mu_g+\Delta \equiv \Delta\mu+\Delta$. In the derivation we assume finite temperature, but most of the results will only be quoted for $T=0$.

A. Homogeneous case

The assumption of spatial homogeneity is appropriate when the atoms are confined in a trap potential that changes very little compared to characteristic quantities of the system, such as the coherence length and the size of the Cooper pairs. In the present context, this assumption is also valid when the laser profile is chosen so that it only probes the middle of the trap where the order parameter is nearly constant in space; this will be discussed in more detail in Sec. VI.

In the homogeneous case the fermion fields $\psi_{e/g}$ can be expanded into plane waves. The Hamiltonian becomes

$$H=H_e+H_{gg'}+\frac{\Delta}{2}\sum_k [c_k^{e\dagger}c_k^e-c_k^{g\dagger}c_k^g] + \sum_{kl} [T_{kl}c_k^{e\dagger}c_l^g+\text{H.c.}], \tag{6}$$

where

$$T_{kl}=\frac{1}{V}\int d^3x\Omega(\mathbf{x})e^{i\mathbf{k}\cdot\mathbf{x}}e^{-i\mathbf{l}\cdot\mathbf{x}}.$$

We calculate the current

$$I=-\langle\dot{N}_e\rangle=-i\langle[H,N_e]\rangle \tag{7}$$

treating H_T as a perturbation: terms of higher order than H_T^2 are neglected. Because we are interested in the current between the superconducting and normal states, correlations of the form $\langle c_e^\dagger c_e^\dagger c_g c_g\rangle$ (and H.c.) are omitted since they correspond to tunneling of pairs (Josephson current). The current can be written

$$I=\int_{-\infty}^{\infty}dt\,\theta(t)\{e^{-i\tilde{\Delta}t}\langle[A^\dagger(0),A(t)]\rangle - e^{i\tilde{\Delta}t}\langle[A(0),A^\dagger(t)]\rangle\}, \tag{8}$$

where $A(t)=\Sigma_{kl}T_{kl}c_k^{g\dagger}(t)c_l^e(t)$ and $c_l^{e/g}(t)=e^{iKt}c_l^{e/g}e^{-iKt}$, where $K=H-H_T-\mu_eN_e-\mu_gN_g$. The two terms in the above equation have the form of retarded and advanced Green's-functions. These are evaluated using Matsubara Green's functions techniques, which leads to

$$I=\sum_{kl}|T_{kl}|^2\int_{-\infty}^{\infty}\frac{d\epsilon}{2\pi}[n_F(\epsilon)-n_F(\epsilon+\tilde{\Delta})] \times A_g(k,\epsilon+\tilde{\Delta})A_e(l,\epsilon), \tag{9}$$

where $n_F(\varepsilon)=1/(e^{\beta\varepsilon}+1)$ is the Fermi distribution function and $A_{g/e}$ are the spectral functions for the superconducting and normal states. We use the standard expressions [25]

$$A_e(l,\epsilon)=2\pi\delta(\epsilon-\xi_l)$$

and

$$A_g(k,\epsilon+\tilde{\Delta})=2\pi[u_k^2\delta(\epsilon+\tilde{\Delta}-\omega_k)+v_k^2\delta(\epsilon+\tilde{\Delta}+\omega_k)].$$

Here $\xi_l=E_l-\mu_e$, where E_l is the energy for a free particle of momentum l and u_k, and v_k and ω_k are given by the Bogoliubov transformation. Here we consider for simplicity the term proportional to v_k^2; u_k^2 is analogous. The laser field is chosen to be a running wave, that is, $\Omega(\mathbf{x})=\Omega e^{i\mathbf{k_L}\cdot\mathbf{x}}$. The term $|T_{kl}|^2$ now produces a δ-function enforcing momentum conservation. Note that this is very different from the assumption of a constant transfer matrix ($\Sigma_{kl}|T_{kl}|^2\rightarrow|T|^2\Sigma_{kl}$) made in the standard calculation for tunneling of electrons over a superconductor—normal metal surface [25]. The final result becomes (assuming for simplicity that the temperature $T=0$)

$$I=-\pi\Omega^2\rho(\Delta)\theta(-\tilde{\Delta}-\omega_{\tilde{k}-k_L}-\Delta\mu) \times\frac{\omega_{\tilde{k}-k_L}-\xi_{\tilde{k}-k_L}}{\omega_{\tilde{k}-k_L}+\xi_{\tilde{k}-k_L}\left[1-\frac{k_L}{\tilde{k}}\right]}, \tag{10}$$

where $\tilde{k}$ is given by the following energy conservation condition:

$$-\tilde{\Delta}+\omega_{\tilde{k}-k_L}+\xi_{\tilde{k}-k_L}=0,$$

$\omega_k=\sqrt{\xi_k^2+\Delta_G^2}$, and

$$\rho(\Delta)=\frac{V}{2\pi^2}\sqrt{\frac{\Delta_G^2-\Delta^2}{\Delta}+2\mu_g} \tag{11}$$

is the density of states, which appears when the summation over momenta is changed into an integration over energies.

The laser momentum k_L can be very small compared to the momentum of the atoms, especially in the case of a Raman process. By setting $k_L=0$, the result becomes, including now terms proportional to both v_k^2 and u_k^2,

$$I=\pm\pi\Omega^2\rho(\Delta)\theta(\Delta^2-\Delta_G^2+2\Delta\mu\Delta)\frac{\Delta_G^2}{\Delta^2}, \tag{12}$$

where $\pm$ are for $\Delta>0$ and $\Delta<0$, respectively. The term with the $-$ sign corresponds to $\Delta<0$, i.e., current from $|g\rangle$ to $|e\rangle$, and the positive term corresponds to current from $|e\rangle$ to $|g\rangle$.

To understand the results in terms of physics, let us first consider the case of equal chemical potentials $\Delta\mu=0$:

$$I=-\pi\Omega^2\frac{\Delta_G^2}{\Delta^2}\rho(\Delta)[\theta(-\Delta-\Delta_G)-\theta(\Delta-\Delta_G)]. \quad (13)$$

In order to transfer one atom from the state $|g\rangle$ to $|e\rangle$, the laser has to break a Cooper pair. The minimum energy required for this is the gap energy Δ_G, therefore the current does not flow before the laser detuning provides this energy; this is expressed by the first step function in Eq. (13). As $|\Delta|$ increases further, the current will decrease quadratically. This is because the case $|\Delta|=\Delta_G$ corresponds to the transfer of particles with $p=p_F$, whereas larger $|\Delta|$ means larger momenta, and there are simply fewer Cooper pairs away from the Fermi surface. This behavior is very different from the electron tunneling where the current grows as $\sqrt{(eV)^2-\Delta_G^2}$ [25] (the voltage eV corresponds to the detuning Δ in our case) because all momentum states are coupled to each other. The second step function in Eq. (13) corresponds to tunneling into the superconductor. In this case, one has to provide extra energy because a single-particle tunneling into a superconductor becomes a quasiparticle excitation with the minimum energy given by the gap energy.

When the chemical potentials are not equal, the situation is more complicated, but the basic features are the same: (i) threshold for the onset of the current determined by the gap energy and difference in chemical potentials, and (ii) further decay of the current because the density of the states that can fulfill energy and momentum conservation decreases.

B. Harmonic confinement

In the case of harmonic confinement, the spatial dependence of the current is nontrivial. We define the total current as

$$I(t)=-\int d^3x\langle\dot{N}_e(\mathbf{x})\rangle, \quad (14)$$

where

$$\dot{N}_e(\mathbf{x})=i[H,N_e(\mathbf{x})]=i[\Omega^*(\mathbf{x})\psi_g^\dagger(\mathbf{x})\psi_e(\mathbf{x})-\text{H.c.}]. \quad (15)$$

No expansion in the plane waves or other basis functions is made at this point and the first-order perturbation calculation leads to a result with explicitly spatially dependent correlation functions:

$$I=2\,\text{Im}[X_{\text{ret}}(-\tilde{\Delta})], \quad (16)$$

where

$$X_{\text{ret}}(-\tilde{\Delta})=i\int_{-\infty}^{\infty}dt\,e^{-i\tilde{\Delta}t}\theta(t)\int d^3x \times\int d^3x'\langle[A^\dagger(\mathbf{x},0),A(\mathbf{x}',t)]\rangle \quad (17)$$

and

$$A(\mathbf{x},t)=\Omega^*(\mathbf{x})\psi_g^\dagger(\mathbf{x})\psi_e(\mathbf{x}). \quad (18)$$

The retarded Green's function $X_{\text{ret}}(-\tilde{\Delta})$ is calculated using Matsubara techniques. To perform the Matsubara summations, the spatially dependent Green's functions for the normal and the superfluid state are expanded using the trap wave functions $\phi_n(\mathbf{x})$ and the Bogoliubov–de Gennes (BdG) eigenfunctions $u_n(\mathbf{x})$ and $v_n(\mathbf{x})$, respectively. The BdG equations are the standard equations for describing inhomogeneous superconductors [29]. This leads to the result

$$X_{\text{ret}}(-\tilde{\Delta})=\int_{-\infty}^{\infty}\frac{d\epsilon}{2\pi}\int d^3x\int d^3x'\,\Omega^*(\mathbf{x})\Omega(\mathbf{x}') \times[\tilde{A}_e(\mathbf{x},\mathbf{x}',\epsilon)G^g_{\text{adv}}(\mathbf{x}',\mathbf{x},\epsilon+\tilde{\Delta}) + G^e_{\text{ret}}(\mathbf{x},\mathbf{x}',\epsilon-\tilde{\Delta})\tilde{A}_g(\mathbf{x}',\mathbf{x},\epsilon)], \quad (19)$$

where $\tilde{A}_{e/g}$ are defined as

$$\tilde{A}_{e/g}(\mathbf{x},\mathbf{x}',\epsilon)=i[G^{e/g}_{\text{ret}}(\mathbf{x},\mathbf{x}',\epsilon)-G^{e/g}_{\text{adv}}(\mathbf{x},\mathbf{x}',\epsilon)],$$

and

$$G^g_{\text{adv}}(\mathbf{x}',\mathbf{x},\epsilon)=\sum_n\frac{u_n(\mathbf{x}')u_n^*(\mathbf{x})}{\epsilon-\omega_n-i\delta}+\frac{v_n^*(\mathbf{x}')v_n(\mathbf{x})}{\epsilon+\omega_n-i\delta}, \quad (20)$$

$$G^e_{\text{ret}}(\mathbf{x},\mathbf{x}',\epsilon)=\sum_n\frac{\phi_n(\mathbf{x})\phi_n^*(\mathbf{x}')}{\epsilon-\xi_n+i\delta}. \quad (21)$$

In taking the imaginary part of the expression (19), we first collect together all spatially dependent terms, which gives real factors of the form $|\int d^3x\,\Omega(\mathbf{x})u_n(\mathbf{x})\phi_m(\mathbf{x})|^2$ [we also use the fact that the trap wave functions $\phi_m(\mathbf{x})$ are real]. Imaginary parts of the remaining terms give spectral functions in the usual way. The derivation leads to

$$I=-2\pi\sum_{n,m}\left|\int d^3x\,\Omega(\mathbf{x})u_n(\mathbf{x})\phi_m(\mathbf{x})\right|^2 \times[n_F(\omega_n)-n_F(\xi_m)]\delta(\xi_m+\tilde{\Delta}-\omega_n) + \left|\int d^3x\,\Omega(\mathbf{x})v_n^*(\mathbf{x})\phi_m(\mathbf{x})\right|^2[n_F(-\omega_n)-n_F(\xi_m)] \times\delta(\xi_m+\tilde{\Delta}+\omega_n), \quad (22)$$

where n_F is the Fermi distribution function at temperature T, ω_n are the BdG energies for the state $|g\rangle$, and $\xi_m=E_m-\mu_e$, where E_m are the single-particle energies for a trap potential defined by $U_0(\mathbf{x})$ for the state $|e\rangle$. Note that this form does not lead to a simple step-function-type behavior like that in the homogeneous case. Due to the nonorthogonality of the trap and the BdG wave functions, transitions between many quantum numbers are allowed and the total current is the sum of all these.

In the following sections, we use the result (22) to investigate the feasibility of the method as a probe in different

physical situations. The eigenfunctions and values $v_n(\mathbf{x})$ and ω_n are calculated numerically from the BdG equations using the pseudopotential method presented in [28]. We assume for simplicity that the trap has spherical symmetry. The quantum numbers n,m in Eq. (22) then become η,l,m, with l,m being the usual angular momentum quantum numbers. The quasiparticle (QP) energies will only depend on η,l. The method of solving the BdG equations is described in detail in [28].

Note that the above derivation assumes that the BdG equations are solved exactly. One can, however, also use the local-density approximation [30] where the chemical potential of the superconducting state is assumed to have a parametric dependence on position and one solves the equations for the homogeneous case at each $\mathbf{x}$. In this case, the derivation is the same as above but $\mathbf{x}$ is now a parameter and the superfluid state Hamiltonian $H_{gg'}$ depends parametrically on $\mathbf{x}$. We may define $H^{\mathbf{x}}_{gg'}$, which is the standard homogeneous system BCS Hamiltonian but with an effective local chemical potential $\mu^{\mathbf{x}} \equiv \mu - U_0(\mathbf{x})$. The result for the current is identical to Eq. (22) except that now u_n, v_n are actually plane waves but they have a parametric dependence on $\mathbf{x}$ via $\mu^{\mathbf{x}}$, as does ω_n. We may denote the current for a chosen $\mathbf{x}$ as $I^{\mathbf{x}}$. The total current is then the average of $I^{\mathbf{x}}$ for all $\mathbf{x}$.

IV. THE EFFECT OF CHEMICAL POTENTIAL, LASER PROFILE, AND TRAPPING

The behavior of the current is strongly influenced by the choice of the physical parameters. This gives us a convenient way to optimize the probing scheme as well as to investigate interesting physics such as the influence of the harmonic confinement. This is our twofold aim in the following.

Although, for instance, the laser profile can be chosen at will, there are a few basic restrictions in choosing the chemical potentials and the interaction strengths between the atoms in different internal states. In order for a gas of fermionic atoms in two internal states to form Cooper pairs, the interatomic interaction should be large enough and the chemical potentials corresponding to the two states should be very close to each other [12]. This is the condition we assume for $|g\rangle$ and $|g'\rangle$. The state $|e\rangle$ is always assumed to have either negligible interaction with the states $|g\rangle$ and $|g'\rangle$, or a considerably lower chemical potential (smaller number of particles). It turns out that not only the pairing affects the light absorption, but also normal interactions described by the Hartree field are crucial. This is illuminated by a comparison of these two cases of $|e\rangle$ having a negligible scattering length or a small chemical potential.

In real experiments, the gas is trapped in a harmonic potential. We have derived results also for the homogeneous case. These can be used in the case of very large traps and they also give a simple intuitive picture of the basic physics in this system. We will show that indeed the trapping has a considerable effect on the results. On the other hand, an effectively homogeneous situation can be achieved by having the laser probe only the center of the trap. As will be shown, this avoids certain problems arising from the nonhomogeneous potential and can give a very clear signature of the superconducting state.

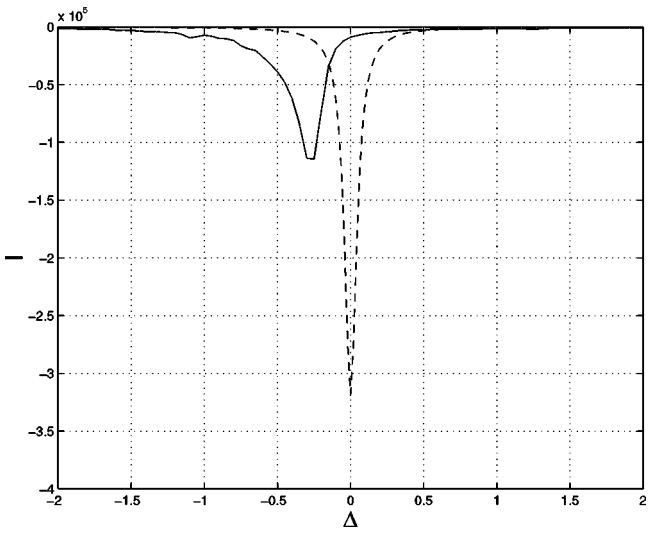

FIG. 2. The current $I=-\langle \dot{N}_e \rangle$ as a function of the laser detuning Δ for $\mu_g=31.5$, $\mu_e=0$ (in units of ω) and $g_{eg}+g_{eg'}=g_{gg'}$. The dashed line correponds to the normal-normal current and the solid one is the normal-superconductor current, for which the peak becomes asymmetric and is shifted.

V. CONSTANT BEAM PROFILE

In this section, we present exact numerical results in the limit when the laser beam intensity can be well approximated by a constant. That is, we take $\Omega(\mathbf{x})=\Omega$ in Eq. (22). As the typical effective wavelength for the laser is much larger than the extent of the trap for the relevant energies, such an approximation should be good as long as the laser amplitude is constant over the whole extent of the cloud. We present results for two situations: the case in which there are no atoms initially in the state $|e\rangle$ and the case in which the chemical potentials for $|e\rangle$ and $|g\rangle$ are the same.

A. No $|e\rangle$ atoms initially

In the case considered in this subsection, we assume that we have initially only a gas of interacting $|g\rangle$ and $|g'\rangle$ atoms. The laser beam then induces transitions to the hyperfine level $|e\rangle$. To obtain clear results, we will assume that the $|e\rangle$ atoms see the same Hartree field as the $|g\rangle$ atoms. This means that $g_{eg}+g_{eg'}=g_{gg'}$ since the $|e\rangle$ atoms see the Hartree field from both the $|g\rangle$ and $|g'\rangle$ atoms. Here, $g_{gg'}=4\pi a_{gg'}/m$ denotes the interaction strength between the two hyperfine states $|g\rangle$ and $|g'\rangle$ and likewise for g_{eg} and $g_{eg'}$. The parameter $a_{gg'}$ is the usual s-wave scattering length for scattering between $|g\rangle$ and $|g'\rangle$ atoms. Experimentally, this situation could possibly be achieved by manipulating an external magnetic field, thereby tuning the effective low-energy interaction between the relevant hyperfine states to an appropriate value. In Fig. 2, we show a typical example of the current $I(\Delta)=-\langle \dot{N}_e \rangle$. We have used parameters such that $g_{gg'}=-l_{\mathrm{ho}}^3\omega$, $\mu_g=31.5\omega$, and the temperature $T=0$, with μ_g denoting the chemical potential for the $|g\rangle$ and $|g'\rangle$ atoms. Here $l_{\mathrm{ho}}=(m\omega)^{-1/2}$ is the harmonic-oscillator length. For ^{6}Li atoms with $a_{gg'}=-1140$ Å [31],

this corresponds to $\sim 1.6\times 10^4$ atoms trapped in the states $|g\rangle$ and $|g'\rangle$ with a trapping frequency of 820 Hz yielding a critical temperature $T_c \sim 110$ nK for the BCS transition. We have added an imaginary part $\Gamma = 0.1\omega$ to the quasiparticle energies such that the $\pi\delta(x)$ functions in Eq. (22) become Lorentzians, $\Gamma/2(x^2+\Gamma^2/4)$.

Normal-normal current. The dashed curve in Fig. 2 depicts the current when the $|g\rangle$ and $|g'\rangle$ atoms are in the normal phase. Since the $|e\rangle$ atoms see the same Hartree field as the $|g\rangle$ atoms and both of them are in the normal phase, the spatial part of the QP wave functions is the same for the two hyperfine states, that is, u_n and v_n are replaced by trap potential wave functions. Because u_n and v_n correspond to the probability of occupation on different sides of the Fermi energy, one has to do the replacement in the following way: for $\xi_n<0$, v_n becomes the trap wave function ϕ_n, $\omega_n = |\xi_n|$, and $u_n=0$, whereas for $\xi_n>0$, we have $v_n=0$, $u_n = \phi_n$, and $\omega_n=\xi_n$. Assuming constant beam profile $[\Omega(\mathbf{x}) \rightarrow \Omega]$, Eq. (22) then reads

$$I = -2\pi\Omega^2 \sum_{n,m} \left| \int d^3x\, \phi_n^*(\mathbf{x})\phi_m(\mathbf{x}) \right|^2 \times [n_F(\xi_n) - n_F(\xi_m)]\delta(\xi_m + \tilde{\Delta} - \xi_n).$$

Energies for the states $|g\rangle$ and $|e\rangle$ were defined respective to their chemical potentials, that is, $\xi_m = E_m - \mu_e$ and $\xi_n = E_n - \mu_g$, thus because $\tilde{\Delta} = \Delta + \Delta\mu$ (also, now $\mu_e = 0$), the chemical potential dependence inside the δ functions vanishes. The overlap integrals of the trap wave functions produce δ_{nm} functions, and the summation over one of the indices gives a simple expression with δ functions of the form $\delta(\Delta)$. The remaining summing over the quasiparticle spectrum (at $T=0$) and replacing $\delta(\Delta)$ by a Lorentzian leads to

$$I(\Delta) = -2\Omega^2 N_g \frac{\Gamma/2}{\Delta^2 + \Gamma^2/4}, \tag{23}$$

where N_g is the number of $|g\rangle$ atoms trapped. One can also derive this expression from the derivation of Eq. (12) for the homogeneous case. Taking the expressions for A_g and A_e and performing the integration over the energy ϵ removes one of the δ functions, leading to an expression that is the same as Eq. (22) but with u_n, v_n, and ϕ_m replaced by plane-wave functions. Then one can continue the derivation as explained above.

Superconductor-normal current. The solid curve in Fig. 2 depicts the current when $|g\rangle$ and $|g'\rangle$ are in the superfluid phase. We see that the maximum of the current is displaced from $\Delta=0$ and that the shape of the current profile is asymmetric. Both effects are quite straightforward to understand. The asymmetry reflects the fact that the current now is given by a sum of Lorentzians centered at different frequencies since the QP spectra for $|g\rangle$ and $|e\rangle$ are different and the overlap integral in Eq. (22) does not give a simple selection rule. The shift in the center of the peak to negative Δ is due to the fact that in order to induce a transition from a low-lying QP state in the superfluid, one needs to break a Cooper pair. This requires an additional energy given by the pairing energy of the QP state. As a fraction $\sim T_c/T_F$ of the particles participates in the pairing and they have on average the pairing energy T_c, one can estimate the order of magnitude of the shift in the center of the peak away from its normal phase value $\Delta=0$ to be $O(T_c^2/T_F)$. Here, T_c is the critical temperature for the BCS transition and $k_B T_F = \mu_g$ is the Fermi temperature for the $|g\rangle$ atoms. For the present parameters, we have $k_B T_c \approx 2.8\omega$, giving $T_c^2/T_F \sim 0.25$ in qualitative agreement with the results depicted in Fig. 2. We have performed numerical calculations for several values $g_{gg'}$ and μ_g, and we find the general behavior as described in the present example. In all the tested cases, the current peak for the superfluid phase is shifted away to negative values of Δ and the shape of the peak is asymmetric as opposed to the simple Lorentzian shape for the normal phase. The shift of the peak is of the order $O(T_c^2/T_F)$.

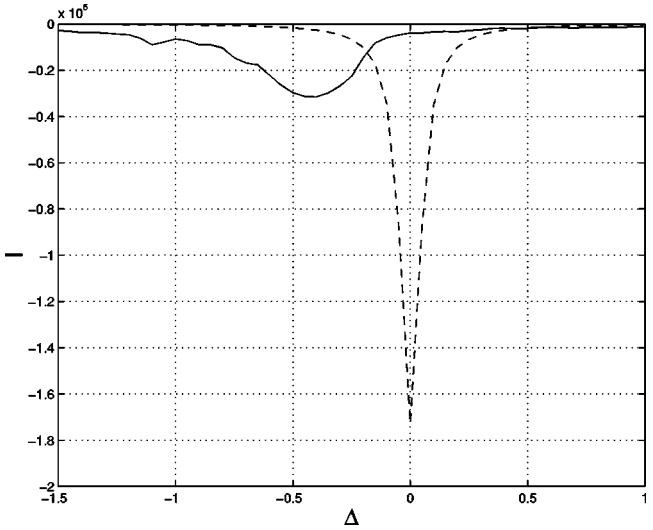

FIG. 3. The current $I = -\langle \dot{N}_e \rangle$. The solid/dashed lines are for the $|g\rangle$ and $|g'\rangle$ atoms in the superfluid/normal phase for $\mu_g = 31.5$, $\mu_e = 21.5$ (trap units), and interactions $g_{eg} + g_{eg'} = g_{gg'}$. The asymmetry and the shift in the peak in the superfluid phase compared to the normal phase are more pronounced than in Fig. 2.

In order to enhance the effect of the pairing on $I(\Delta)$ even further, one could initially also trap some $|e\rangle$ atoms. As long as $\mu_g - \mu_e \gg \Delta_G$, the $|e\rangle$ atoms will not Cooper-pair with the $|g\rangle$ or $|g'\rangle$ atoms even though g_{eg} or $g_{eg'} < 0$ [12]. By having the lower QP states for the $|e\rangle$ atoms filled, there will only be transitions between the QP states around the Fermi energy. Since these states are influenced the most by the pairing, the effect of the superfluidity on $I(\Delta)$ will be even stronger than for the parameters relevant for Fig. 2. This is illustrated by Fig. 3, where we plot $I(\Delta)$ for the same parameters as above apart from the fact that now $\mu_e = 21.5\omega$. We see that both the asymmetry and the shift in the peak in the superfluid phase as compared to the normal phase are more pronounced than in Fig. 2. This is simply because the transitions deep below the Fermi level, which are essentially immune to the effects of superfluidity, are blocked by filling up the levels for the $|e\rangle$ atoms up to the energy $E = 21.5\omega$. However, it might be somewhat more difficult to achieve this

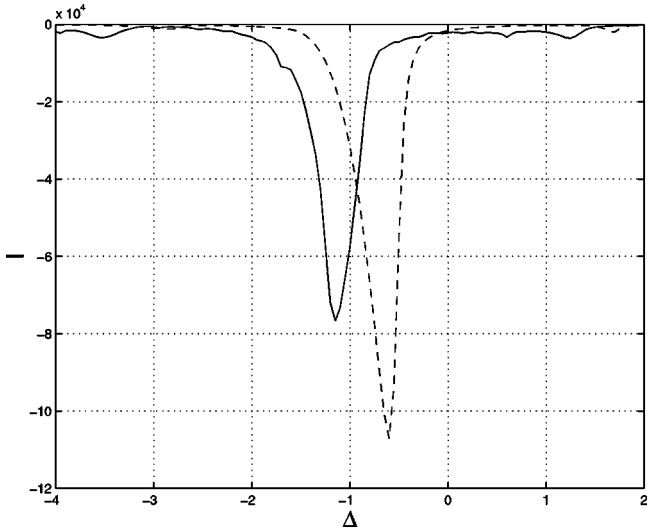

FIG. 4. The current $I=-\langle \dot{N}_e \rangle$. The solid/dashed lines are for the $|g'\rangle$ and $|g\rangle$ atoms in the superfluid/normal phase for $\mu_g=31.5$, $\mu_e=0$ (trap units), and $g_{eg}+g_{eg'}=0.9g_{gg'}$. The current profile is shifted and asymmetric for both the normal and superconducting phase, but pairing enhances both effects.

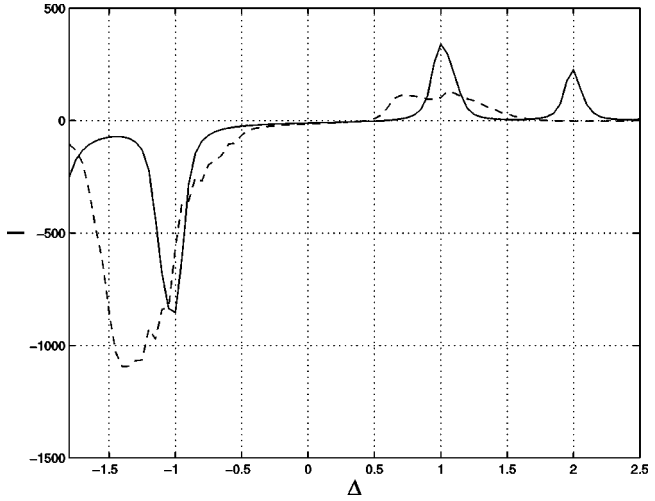

FIG. 5. The current $I=-\langle \dot{N}_e \rangle$. The solid/dashed lines are for the $|g'\rangle$ and $|g\rangle$ atoms in the superfluid/normal phase. Here $\mu_g=\mu_e=31.5$ (trap units) and $g_{eg}=g_{eg'}=0$. The peaks correspond to individual QP energy bands overlapping.

situation experimentally, as it requires the initial trapping of three (instead of two) hyperfine states with a rather good control of the populations in each state.

One should note that it is important that the Hartree field seen by the $|g\rangle$ and $|e\rangle$ atoms is approximately the same. Otherwise, the wave functions and the spectra for the $|g\rangle$ and $|e\rangle$ atoms will be different even when the $|g\rangle$ and $|g'\rangle$ atoms are in the normal phase. The overlap integrals will then not give simple selection rules and there will be a contribution from many Lorentzians centered in general away from $\Delta=0$. Consequently, $I(\Delta)$ will not be given by the simple formula in Eq. (23). This is illustrated in Fig. 4, where we plot the current $I(\Delta)$ for the same parameters as given above (with no $|e\rangle$ atoms initially), apart from which we now have $g_{eg}+g_{eg'}=0.9g_{gg'}$. As expected, the current profile is shifted away from $\Delta=0$ and is asymmetric, even when the $|g\rangle$ and $|g'\rangle$ atoms are in the normal phase. The shift to negative frequencies is easy to understand: The attractive mean (Hartree) field seen by the $|e\rangle$ atoms is smaller than the attractive field seen by the $|g\rangle$ atoms since $g_{eg}+g_{eg'}=0.9g_{gg'}$. Therefore, the trap states for the $|e\rangle$ atoms in general have a slightly higher energy than for the $|g\rangle$ atoms, and the normal phase current is shifted to negative Δ. Figure 4 demonstrates that the pairing field still causes a general shift of $I(\Delta)$ to negative frequencies and introduces further asymmetry since the pairing energy still needs to be broken to generate a current from the superfluid phase. This effect is readily visible since the Hartree fields seen by the $|g\rangle$ and $|e\rangle$ atoms are approximately the same for the parameters chosen. However, if the difference in the Hartree fields becomes too large, the spread in the signal is determined by this difference and any additional effects coming from the pairing field are correspondingly obscured. In general, to be able to detect the presence of superfluidity using the scheme described in this section, one should have $\Delta W \ll \Delta_G$, where $\Delta W=|g_{gg'}-g_{eg}-g_{eg'}|\rho$ denotes the difference in the Hartree fields with ρ being the average density of the $|g\rangle$ atoms, and Δ_G is the average gap.

We conclude that if $g_{eg}+g_{eg'}=g_{gg'}$ to a very good approximation so that the difference in the Hartree fields seen by the $|g\rangle$ and the $|e\rangle$ is negligible, the effect of superfluidity on the current $I(\Delta)$ should be straightforward to observe. The current in the normal phase is a simple Lorentzian centered around $\Delta=0$, whereas in the superfluid phase it is asymmetric and shifted away from $\Delta=0$. Furthermore, the shift in the center of the peak provides an estimate of T_c if T_F is known. Both the asymmetry and the shift away from $\Delta=0$ should be easily observable indications of the presence of superfluidity. The effect is further enhanced if one initially traps $|e\rangle$ atoms keeping $\mu_g-\mu_e \gg \Delta_G$. In general, the scheme described in this section requires that the difference in the Hartree fields seen by the $|g\rangle$ and the $|e\rangle$ is smaller than the average pairing field in order to obtain a visible effect of the superfluidity on the current.

B. Equal chemical potentials

We now consider the case of $\mu_e \simeq \mu_g$, where there is initially many atoms trapped in the state $|e\rangle$. Hence, to avoid the otherwise interesting possibility of the $|e\rangle$ atoms participating in the pairing, we assume that $g_{eg}=g_{eg'}=0$. In Fig. 5, we plot the current $I(\Delta)$ for $g_{gg'}=-l_{\rm ho}^3\omega$, $\mu_e=\mu_g=31.5\omega$, $T=0$, and $g_{eg}=g_{eg'}=0$. We have taken $\Gamma=0.1\omega$. As can be seen, there are several peaks in $I(\Delta)$ both when $|g\rangle$ and $|g'\rangle$ are in the normal phase and when they are in the superfluid phase. In both cases, the peaks simply correspond to individual QP energy bands overlapping.

To see this, we plot in Fig. 6 the corresponding lowest QP energies for the $|e\rangle$, $|g\rangle$, and $|g'\rangle$ atoms in both phases as a function of their angular momentum l. As we are in the Bogoliubov picture, all QP energies are positive and measured relative to the chemical potential. In the normal phase, nega-

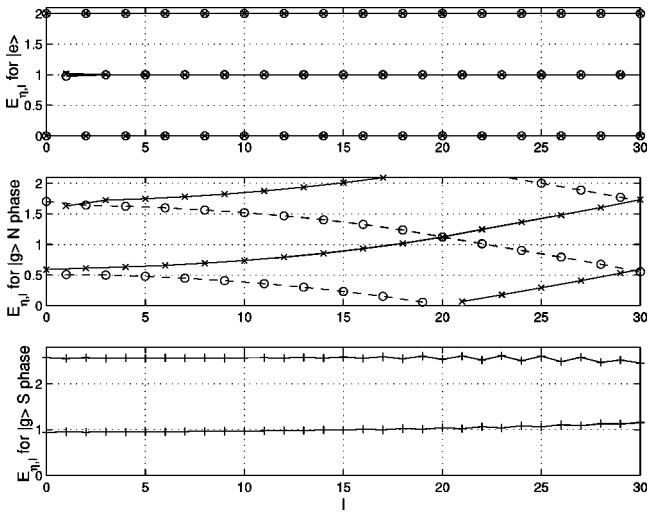

FIG. 6. The lowest QP energies $E_{\eta,l}$ as a function of the angular momentum l; parameters are the same as in Fig. 4.

tive QP energies $\xi_n=\epsilon_n-\mu<0$ are represented as positive QP energies $E_n=|\xi_n|$ with hole character. In Fig. 6, we label a hole state by $\bigcirc$ whereas a particle state is indicated by $\times$. In the superfluid phase, the QP's are in general a superposition of a hole and a particle, which we label by $+$.

We see that when the Hartree field is attractive, a normal phase energy band with a downward curvature in Fig. 6 is a hole band whereas a normal phase energy band with an upward curvature is a particle band. The reason is that particle states with lower angular momentum l have a lower energy for an attractive interaction ($g<0$) than states with a higher l since the wave function overlap with the Hartree field decreases with increasing l [4].

The QP bands for the $|e\rangle$ atoms are flat as they are the simple unperturbed harmonic-oscillator states with energies $E_n=|(n+3/2)\omega-\mu_e|$. The lowest $E=0$ band corresponds to the harmonic-oscillator states at the chemical potential ($n=30$) with angular momentum $l=0,2,\ldots,30$. The interpretation of the spectra is described in detail in [4,20]. There is a one-to-one correspondence between the peaks in Fig. 5 and the QP bands depicted in Fig. 6. For instance, the broad peak centered around $\Delta=\omega$ when the $|g\rangle$ and $|g'\rangle$ atoms are in the normal phase corresponds to transitions from the half-filled QP band at $E=0$ for the $|e\rangle$ atoms into the empty (particle) band with $0.5\lesssim E/\omega\lesssim 1.8$ for $l=0,2,\ldots,30$ for the $|g\rangle$ atoms in the normal phase.

We note that the peaks for the superfluid phase are sharper than the peaks for the normal phase. This is because the lowest QP bands for the $|g\rangle$ atoms are almost degenerate as a function of l in the superfluid phase, as can be seen from Fig. 6. These states are strongly influenced by the pairing field, which ''pushes'' them away from the center of the trap. They are concentrated in the region between where the pairing field and the trapping potential are significant [18,20], and they thus do not feel the Hartree field. Therefore, their dependence on the quantum number l is much weaker than in the normal phase.

We have performed calculations for a number of different parameters and we have observed the general behavior of $I(\Delta)$ as described above. We conclude that when we have $\mu_e\simeq\mu_g$ and $g_{eg}=g_{eg'}=0$, the presence of superfluidity is somewhat harder to detect as compared to the situation described in Sec. V A. This is because the Hartree field tends to obscure any additional effect coming for the pairing. The current $I(\Delta)$ has in general many peaks corresponding to the energetic overlap between individual QP bands for the $|e\rangle$ and the $|g\rangle$ atoms both for the normal and the superfluid phases. The effect of the superfluidity is to make the peaks sharper than in the normal phase since the pairing field tends to restore the degeneracy in the QP energies with respect to the angular momentum. One could therefore possibly detect the onset of superfluidity as a sharpening of the peaks.

VI. PROBING THE CENTER OF THE TRAP—AN EFFECTIVELY HOMOGENEOUS SYSTEM

We now assume that the laser intensity $\Omega(\mathbf{x})$ is large in the center of the cloud and that it decreases quickly as a function of the distance from the center of the trap. This situation can be experimentally achieved by using a Raman transition scheme with two perpendicular laser beams crossing each other at the center of the cloud. The profile of each laser beam should be narrow on the length scale of the trapped cloud. Since the laser beams then effectively probe only atoms in the center of the cloud where the Hartree and pairing fields are approximately constant, we would expect the observed signal to be well described by the results for a homogeneous system as given by Eq.(12). From Sec. III A, we conclude that, for a homogeneous system, the optimal way of detecting the presence of the pairing field is to have $\mu_g\simeq\mu_e$ [see Eq. (13)]. In this limit, all low-lying transitions far away from the Fermi energy and thus very little affected by the pairing are Fermi blocked. The transitions contributing to $I(\Delta)$ are all close to the Fermi level and hence strongly influenced by the presence of the pairing field. We will therefore concentrate on the case in which the effective chemical potential in the center of the trap is the same for $|g\rangle$ and $|e\rangle$. As we will see, this case opens up the interesting possibility of directly measuring the size of the gap in the center of the cloud.

We use the same set of parameters as in Sec. V B for the $|g\rangle$ and $|g'\rangle$ atoms. But now we assume that the intensity profile for the beam can be well approximated by a sphere of constant intensity for $r\leqslant r_0$ and zero intensity for $r>r_0$, with r denoting the distance to the center of the trap. That is, we take $\Omega(\mathbf{r})=\Omega\Theta(r_0-r)$ in Eq. (22) with $r_0=2l_{\mathrm{ho}}$. From Fig. 7, we see that $\Delta_G(r)\simeq 6\omega$ and $W(r)\simeq 15\omega$ for $r\leqslant 2l_{\mathrm{ho}}$. Thus, the effective local potential for the $|g\rangle$ atoms is $\mu_g\sim 46.5\omega$. We therefore take $\mu_e=46.5\omega$ and $g_{eg}=g_{eg'}=0$ in order to have the same effective local chemical potential for $|g\rangle$ and $|e\rangle$ in the center of the trap. The result is shown in Fig. 8. Since the system is approximately homogeneous for $r\leqslant 2l_{\mathrm{ho}}$, one could expect the current profile to be well described by Eq. (13), with $\mu_e=\mu_g=46.5\omega$ and $\Delta_G=6\omega$. We therefore also plot the result predicted by Eq. (13). Here we take $\mu_e=\mu_g=46.5\omega$ and $\Delta_G=6\omega$ and we have normalized $I(\Delta)$ to a volume of $V=4\pi r_0^3/3$. We have taken a rather large value of $\Gamma=1\omega$ such that the discrete nature of

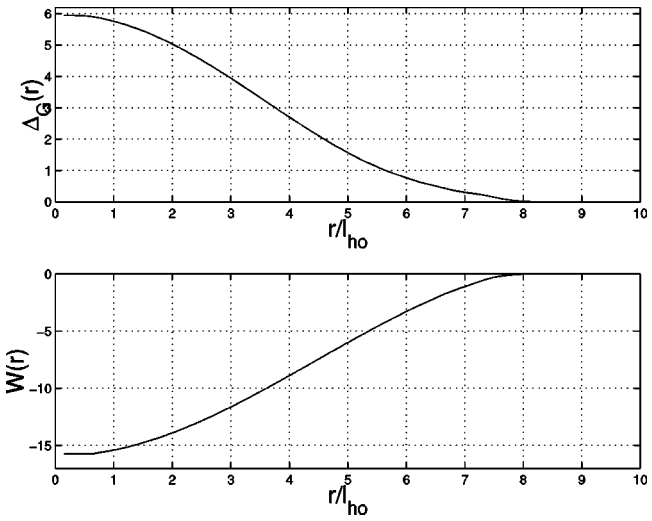

FIG. 7. The pairing field $\Delta_G(r)$ and Hartree field $W(r)=g_{gg'}\langle\psi_g^\dagger\psi_g\rangle$ in units of ω; parameters are the same as in Fig. 4.

the trap spectrum is washed out. Note that a finite imaginary part Γ of the QP energies corresponds to convoluting Eq. (13) with a Lorentzian of width Γ.

As can be seen, there is a good agreement between the exact numerical result and the prediction based on Eq. (13). Especially, the current is zero for $-6\omega\lesssim\Delta\lesssim 6\omega$ as predicted by Eq. (13), since one either needs to break a Cooper pair with pairing energy $\sim\Delta_G(r=0)$ to produce a current into $|e\rangle$ ($\Rightarrow\Delta\lesssim -6\omega$) or one has to create a QP with energy minimum $\sim\Delta_G(r=0)$ ($\Rightarrow\Delta\gtrsim 6\omega$) to generate a current into $|g\rangle$. The peaks in the numerical result reflect, of course, the discreteness of the trap levels. These peaks are quite large, as there are only ≈ 500 particles trapped in the region $r\leqslant 2l_{\rm ho}$ for the parameters given above. Clearly, these peaks cannot be reproduced by the homogeneous treatment given by Eq. (13), which, however, reproduces the general shape of the current profile well. If we had chosen a larger system, the individual peaks would be more numerous and smaller on the scale of the gap $\Delta_G(r=0)$ and the agreement between the homogeneous approximation and the exact result would probably be even better.

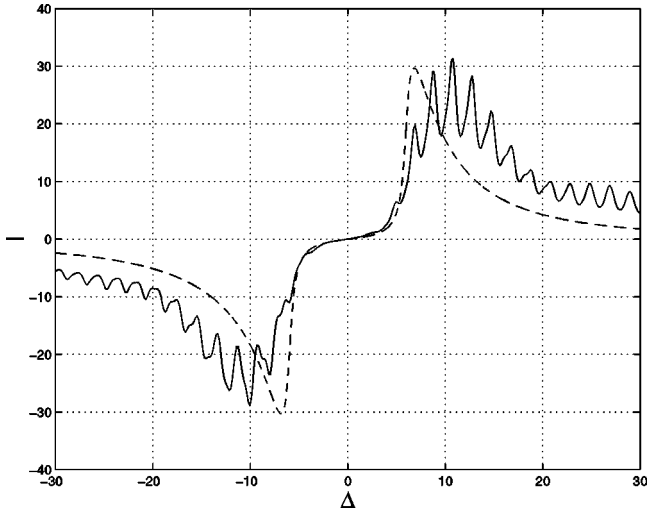

FIG. 8. The current $I=-\langle\dot{N}_e\rangle$ for $\mu_g=\mu_e=46.5$ (trap units) and $g_{eg}=g_{eg'}=0$. The solid line is the numerical result obtained by the inhomogeneous case treatment but with the laser focused on the center of the trap, whereas the dashed line is based on the homogeneous case result Eq. (13), with $\Delta_G=6$.

We conclude that by concentrating the beam intensity to the center of the cloud where the gas can be to a good approximation regarded as homogeneous, the current profile $I(\Delta)$ is well described by the results presented in Sec. III A. An important result is that by adjusting the parameters such that the local chemical potentials are the same $[\mu_g-W_g(r=0)\simeq\mu_e-W_e(r=0)]$, one should be able to measure directly the size of the gap in the center of the cloud. It is simply given by the threshold detuning energy below which the observed current should be zero: for $|\Delta|\lesssim\Delta_G$ the current $I(\Delta)\simeq 0$.

VII. CONCLUSIONS

The observation of the predicted BCS state in gases of trapped atomic fermions poses a double challenge. The order parameter is small, thus a sensitive probe has to be found. Furthermore, the trapping potential leads to the appearance of in-gap low-energy excitations, which may make it difficult to resolve the gap energy. In this paper, we have presented a method based on the transfer of atomic population over a superconductor–normal state interface. This interface is effectively created by using a laser to couple internal states with large and small scattering lengths. The population transfer requires breaking a Cooper pair and the extra energy for this is provided by the laser detuning. The change in the atomic population as a function of the laser detuning thus gives information about the gap energy. We have derived the current of population both in the case of a trapped gas and a homogeneous system, and we investigated the feasibility of the method in different physical regimes.

We found that, in the case of a constant laser profile, the clearest signatures of the BCS state are observed when it is assumed that there are initially no atoms in the normal state. Furthermore, the scattering length between the normal state atoms and the Cooper-paired ones is assumed to be about half of the scattering length between the two Cooper-paired ones; this causes all the atoms to see the same Hartree field. In this physical situation, the effect of the BCS state is particularly simple and clear: the maximum in the current of population as a function of the detuning is shifted and the peak becomes asymmetric. Although this would probably be the optimal choice, other initial conditions and probe parameters lead to clear signatures of the BCS state as well.

To avoid the problems arising from the nonhomogeneous trapping potential, we propose to probe only the middle of the trap. The order parameter is effectively homogeneous in the middle and the wave functions of the in-gap excitations are located away from the center. In practice, this kind of probing can be done by using two orthogonal Raman beams that intersect only in the middle of the trap. We have shown that indeed this leads to a result very similar to the one in the homogeneous case: the maximum of the current is shifted exactly by the amount of the gap energy. This allows a direct measurement of the gap energy.

ACKNOWLEDGMENTS

P.T. and M.R. acknowledge the support of the Academy of Finland (Projects No. 48845, No. 47140, and No. 44897, Finnish Center of Excellence Program 2000–2005). Work at the University of Innsbruck is supported by the Austrian Science Foundation and EU TMR networks. P.T. also acknowledges the European Commission and the University of Innsbruck for financial support.

[1] B. DeMarco and D.S. Jin, Science **285**, 1703 (1999).
[2] M.-O. Mewes, G. Ferrari, F. Schreck, A. Sinatra, and C. Salomon, Phys. Rev. A **61**, 011403(R) (2000).
[3] K.M. O'Hara, M.E. Gehm, S.R. Granade, S. Bali, and J.E. Thomas, Phys. Rev. Lett. **85**, 2092 (2000).
[4] G. M. Bruun and K. Burnett, Phys. Rev. A **58**, 2427 (1998).
[5] Tin-Lun Ho and C. V. Ciobanu, Phys. Rev. Lett. **85**, 4648 (2000).
[6] G. M. Bruun and C. W. Clark, Phys. Rev. Lett. **83**, 5415 (1999).
[7] L. Vichi and S. Stringari, Phys. Rev. A **60**, 4734 (1999).
[8] A. Csordás and R. Graham, Phys. Rev. A **63**, 013606 (2001).
[9] G. Ferrari, Phys. Rev. A **59**, R4125 (1999); L. Vichi, J. Low Temp. Phys. **121**, 177 (2000).
[10] J. Ruostekoski and J. Javanainen, Phys. Rev. Lett. **82**, 4741 (1999).
[11] T. Busch, J. R. Anglin, J. I. Cirac, and P. Zoller, Europhys. Lett. **44**, 1 (1998).
[12] H.T.C. Stoof, M. Houbiers, C.A. Sackett, and R.G. Hulet, Phys. Rev. Lett. **76**, 10 (1996).
[13] L. You and M. Marinescu, Phys. Rev. A **60**, 2324 (1999).
[14] For recent reviews, see E.A. Cornell, J.R. Ensher, and C.E. Wieman, in Conference Proceedings of the Enrico Fermi Summer School on Bose-Einstein Condensation, Varenna, Italy (1998) (unpublished); W. Ketterle, D.S. Durfee, and D.M. Stamper-Kurn, *ibid.*
[15] F. Weig and W. Zwerger, Europhys. Lett. **49**, 282 (2000).
[16] W. Zhang, C.A. Sackett, and R.G. Hulet, Phys. Rev. A **60**, 504 (1999).
[17] J. Ruostekoski, Phys. Rev. A **60**, R1775 (1999).
[18] M.A. Baranov, JETP Lett. **70**, 396 (1999).
[19] M.A. Baranov and D.S. Petrov, Phys. Rev. A **62**, 041601(R) (2000).
[20] G.M. Bruun and C.W. Clark, J. Phys. B **33**, 3953 (2000).
[21] F. Zambelli and S. Stringari, Phys. Rev. A **63**, 033602 (2001).
[22] A. Minguzzi and M.P. Tosi, Phys. Rev. A **63** 023609 (2001).
[23] K.G. Petrosyan, JETP Lett. **70**, 11 (1999).
[24] P. Törmä and P. Zoller, Phys. Rev. Lett. **85**, 487 (2000).
[25] G.D. Mahan, *Many-Particle Physics* (Plenum Press, New York, 1990).
[26] J.L. Bohn, Phys. Rev. A **61**, 053409 (2000).
[27] J. Williams, R. Walser, J. Cooper, E. Cornell, and M. Holland, Phys. Rev. A **59**, R31 (1999).
[28] G. Bruun, Y. Castin, R. Dum, and K. Burnett, Eur. Phys. J. D **7**, 433 (1999).
[29] P.G. de Gennes, *Superconductivity of Metals and Alloys* (Addison-Wesley, New York, 1989).
[30] M. Houbiers, R. Ferwerda, H.T.C. Stoof, W.I. McAlexander, C.A. Sackett, and R.G. Hulet, Phys. Rev. A **56**, 4864 (1997).
[31] E. R. I. Abraham, W. I. Alexander, J. M. Gerton, R. G. Hulet, R. Coté, and A. Dalgarno, Phys. Rev. A **55**, R3299 (1997).